

5]). The dynamical pressure balance between the ionized and neutral phases is then reestablished by means of a shock wave (SW) that propagates into the CG. Indeed, high-density gas observations show the signature of a SW along the edge of all sources, propagating into the molecular gas (Fig. 2). This situation is best seen in TC0 where only the external layers have undergone the SW compression (Fig. 1, A to D). Only 1.2×10^5 years after the ionization began (on a time scale comparable to the age of the Trifid) the simulated CG has evolved toward a morphology similar to that of TC2; the SW preceding the ionization front has induced the formation of a dense core. This core is 20 to 30 times as dense as the main unperturbed body of gas and contains the bulk of the mass of the CG. This appears to be similar to what we observe toward TC2 (Fig. 1C). We find that such conditions tend to destabilize the gravitational equilibrium of TC2. Before being exposed to the UV flux, the cloud was close to virial equilibrium (the ratio of its actual mass to the virial mass is ≈ 2 to 3). The change in surface pressure decreases the maximum mass that can be maintained in equilibrium against its gravity and the external pressure (Ebert-Bonnor mass) to $0.25 M_{\odot}$. The actual mass of TC2 is so high above this limit that the large-scale cloud collapse cannot be halted. Simultaneously, the gravitational free-fall time decreases from 2×10^5 years (for a mean density of $2 \times 10^5 \text{ cm}^{-3}$, similar to that of TC2) to a few 10^4 years for the dense core, enabling or accelerating the gravitational collapse. Despite the observational evidences of gravitational collapse and radiatively driven implosion of TC2, we cannot ascertain that the gravitational collapse was triggered by the ionization front. However, the protostar is so young that there has been interaction between both processes.

Scaled at the distance of the nearby molecular cloud complexes (~ 160 pc) where all the class 0 sources have been discovered, the fluxes of TC1 to TC4 are one order of magnitude larger than those of the other class 0 sources. The sources in the Trifid are also more massive (Table 1) than most of the known class 0 candidates, which have masses of about $1 M_{\odot}$. Comparison with the $\text{HCO}^+ J = 1-0$ line (Fig. 1, A and B) indicates that the dust cores TC0 to TC4 contain most of the mass of dense material surrounding the ionized bubble, a large fraction of which is used in the formation of the protostars. Hence, TC1 to TC4 probably signal the end of the second generation of star formation in the Trifid while leaving little dense material available for subsequent episodes. TC1 to TC4 are the first massive young stellar objects that are neither observed in warm molecular clouds like the Orion nebula nor associated with bright near-IR emission. The typical distance between the different protostars in the Trifid is similar to

that of O stars in more evolved HII regions, like the Rosette nebula. These massive sources may evolve toward O stars or clusters of lower mass stars. Once these stars have emerged from their cocoons, they will increase the UV flux impinging on the remaining low-density gas and will accelerate the creation of a large HII region with its own cluster of OB stars similar to those of the Rosette and other HII nebulae.

References and Notes

1. A. A. Blaauw, *Annu. Rev. Astron. Astrophys.*, **2**, 213 (1964).
2. B. G. Elmegreen and C. J. Lada, *Astrophys. J.* **214**, 725 (1977).
3. K. Sugitani, Y. Fukui, A. Mizuno, N. Ohashi, *ibid.* **342**, L87 (1989).
4. J. Cernicharo, R. Bachiller, G. Duvert, Gonzalez-Alfonso, E. Gomez-Gonzalez, *J. Astron. Astrophys.* **268**, 589 (1992).
5. B. Lefloch and B. Lazareff, *Astron. Astrophys.* **289**, 559 (1994).
6. C. J. Lada, *Annu. Rev. Astron. Astrophys.* **23**, 267 (1985).
7. B. T. Lynds, B. J. Canzian, E. J. O'Neil Jr., *Astrophys. J.* **288**, 164 (1985).
8. A. P. Whitworth, A.S. Bhattal, S. J. Chapman, M. J. Disney, J. A. Turner, *Mon. Not. R. Astron. Soc.* **268**, 291 (1994).
9. M. Kessler *et al.*, *Astron. Astrophys.* **315**, L27 (1996).
10. C. Cesarsky *et al.*, *ibid.*, p. L32.
11. D. Lemke *et al.*, *ibid.*, p. L64.
12. B. Reipurth, *A General Catalogue of the Herbig-Haro*

Objects. Available at www-astro.phast.umass.edu/catalogs/HHcat.

13. J. Cernicharo *et al.*, in *Herbig Haro Objects and The Birth of Low-Mass Stars*, A. Castets and F. Malbet, Eds. (Kluwer, Dordrecht, Netherlands, 1997), pp. 8–11.
14. Ph. André, D. Ward-Thompson, M. Barsony, *Astrophys. J.* **406**, 122 (1993).
15. Ph. André and T. Montmerle, *ibid.* **420**, 837 (1994).
16. Observations were made with ISO, an ESA project with instruments funded by ESA member states (especially the PI countries: France, Germany, the Netherlands, and the United Kingdom) and with the participation of Institute of Space and Astronautical Science and NASA. The ISOCAM data presented in this paper were analyzed with CIA, a joint development by the ESA Astrophysics Division and the ISOCAM Consortium led by the ISOCAM principal investigators, C. Cesarsky, Direction des Sciences de la Matière, Commissariat à l'Energie Atomique, France. The Nordic Optical Telescope (NOT) is operated on the island of La Palma by the NOT Scientific Association in the Spanish Observatorio del Roque de los Muchachos of the Instituto de Astrofísica de Canarias (IAC), and the IAC80 telescope is operated by the IAC on the island of Tenerife in its Observatorio del Teide. The National Radio Astronomy Observatory (VLA) is operated by Associated Universities under cooperative agreement with the NSF. J.C. thanks the Spanish Dirección General de la Enseñanza Superior for support through ACP96-0168, ESP96-2529-E, and PB96-0083. We thank B. Reipurth, G. Pérez, F. Boulanger, J. L. Rasilila, M. Guerrero, M. Centurión, and R. Corradi for their help and for useful comments and suggestions.

27 January 1998; accepted 14 September 1998

Exceeding 5000-Fold Concentration of Dilute Analytes in Micellar Electrokinetic Chromatography

Joselito P. Quirino* and Shigeru Terabe

When a neutral analyte zone is injected into a charged pseudostationary phase, the length of the zone is predicted to be narrowed by $1/(1+k)$, where k is the retention factor. The conditions for zone narrowing to occur assume negligible electroosmotic flow, a relatively constant electric field along the capillary column, and no pseudostationary phase in the injected analyte mixture. The theoretically expected concentration enhancement was demonstrated experimentally. Consequently, the detection sensitivity of analytes in micellar electrokinetic chromatography (MEKC) can be improved significantly. For example, 9 to 18 parts per billion of an environmentally important racemic herbicide spiked in lake water was separated by MEKC and detected by ultraviolet absorption.

Electrokinetic chromatography (EKC), a mode of capillary electrophoresis, is a group of analytical separation techniques named after electrokinetic phenomena that include electroosmosis, electrophoresis, and chromatography (J). EKC offers diverse advantages over other techniques including high efficiency, technical simplicity, applicability to most

analytes, small sample and reagent requirements, and potential for miniaturization (for example, EKC on chips). However, detection sensitivity is rather poor, at the micromolar level with on-line photometric detection. Powerful detectors like laser-induced fluorescence (2) can lower detection sensitivity several orders but are not widely applicable and are too expensive for many laboratories. On-line concentration by transient isotachopheresis (3) and sample stacking (4, 5) have also been demonstrated to solve this problem, which provided at most hundredfold increas-

Faculty of Science, Himeji Institute of Technology, Kamigori, Hyogo, Japan 678-1297.

*To whom correspondence should be addressed. E-mail: jquirino@sci.himeji-tech.ac.jp

REPORTS

es in detection. Here, we show the exceptional narrowing of neutral analyte zones in EKC under constant electric fields, which in theory can provide an almost unlimited increase in detection sensitivity. With the ability to achieve concentration enhancements as reported here, many problems in chemical analysis might be surmounted. Moreover, the fate of zones in EKC is given a new perspective.

This special concentration effect, which we call sweeping, is a physical phenomenon that works well for all analytes with great affinities toward the pseudostationary phase that is far different from those described in other capillary electrophoresis modes for ionizable (3, 4) and neutral analytes (5). Sweeping in EKC is defined as the picking and accumulating of analytes by the pseudostationary phase that fills the sample zone during application of voltage. It is analogous to using a broom to carefully carry along grains of rice scattered on the floor.

The pseudostationary phase chosen for EKC as an example in this report is the anionic micelle of sodium dodecyl sulfate (SDS), a mode commonly termed micellar electrokinetic chromatography (MEKC) (6). The use of very low pH buffers protonates silanol groups and provides an almost zero electroosmotic flow environment. The analytes are neutral and are prepared in a matrix with the same conductivity as the background solution (BGS). If a sample solution (S) is injected into the open tube or capillary column (Fig. 1A), micelles from the BGS (cathode) will enter the S zone upon application of voltage and sweep neutral analytes into thin concentrated zones (Fig. 1, B and C). Separation of zones is shown in Fig. 1D. The concentration of the micelles entering and retention factors (k) of the analytes are assumed to be near those in the BGS. Here, the retention factor is the ratio of the number of moles of solute in the mobile micellar phase to that in the stationary aqueous phase.

The length of the swept zone (l_{sweep}) is given below (Eq. 1). This is assumed to occur when the first batch of micelles that entered the S zone reaches the interface between S and BGS (I) (see Fig. 1C),

$$l_{\text{sweep}} = d_{\text{mc}} - d_a \quad (1)$$

where the distances traveled by the first batch of micelles that entered the S zone and by neutral analyte molecules that are found farthest from interface I are d_{mc} and d_a , respectively; d_{mc} is simply the length of the zone injected (l_{inj}) and d_a is l_{inj} multiplied by the factor $k/(k+1)$ to incorporate the role of retention factor. Therefore, Eq. 1 is described by using k and l_{inj} (Eq. 2),

$$l_{\text{sweep}} = l_{\text{inj}} (1/1 + k) \quad (2)$$

Swept zones of high k analytes must be nar-

rower than lower k zones. This is illustrated in Fig. 1 (B and C) in the region boxed by green lines; the rightmost red line depicts the molecules of a low retention factor analyte (a_2) and the region boxed by the red lines depicts the molecules of a higher retention factor analyte (a_1). The electropherogram in Fig. 2 shows that peak widths increase and k values decrease from the left to the right peak and that resolution is not greatly affected by sweeping; note the long length of the S zone injected (7). Quantitative verification of Eq.

2 was also done with some aromatic compounds. Given the plug lengths and computed k values (δ) of some phenols, a plot of l_{inj} (x axis) versus l_{sweep} (y axis) for each k is constructed. The predicted lengths agreed well with experimentally determined values. Similar results were obtained with some alkyl phenyl ketones up to heptanophenone ($k = 91$) (9).

Guided by the law of conservation of mass, the resulting concentration after sweeping (C_{sweep}) is given below

Fig. 1. Evolution of analyte zones in EKC under sweeping conditions. (A) Starting situation. Injection of sample solution S with length l_{inj} after conditioning the capillary with BGS (found at both electrode vials). (B) Micelles from the cathodic vial enter the S zone or capillary (area enclosed by blue lines) and sweep the analytes into narrower bands depending on the retention factor ($k_{a1} > k_{a2}$, depicted by red and green lines, respectively). (C) First batch of micelles that entered the S zone reaches the interface between S and BGS zones (I). (D) Separation of zones based on MEKC; other symbols, analytes (a_1, a_2), length of capillary (L), analyte molecules found farthest from I during A (a_1^*, a_2^*), and first batch of micelles that entered S zone after application of voltage at negative polarity (mc^*).

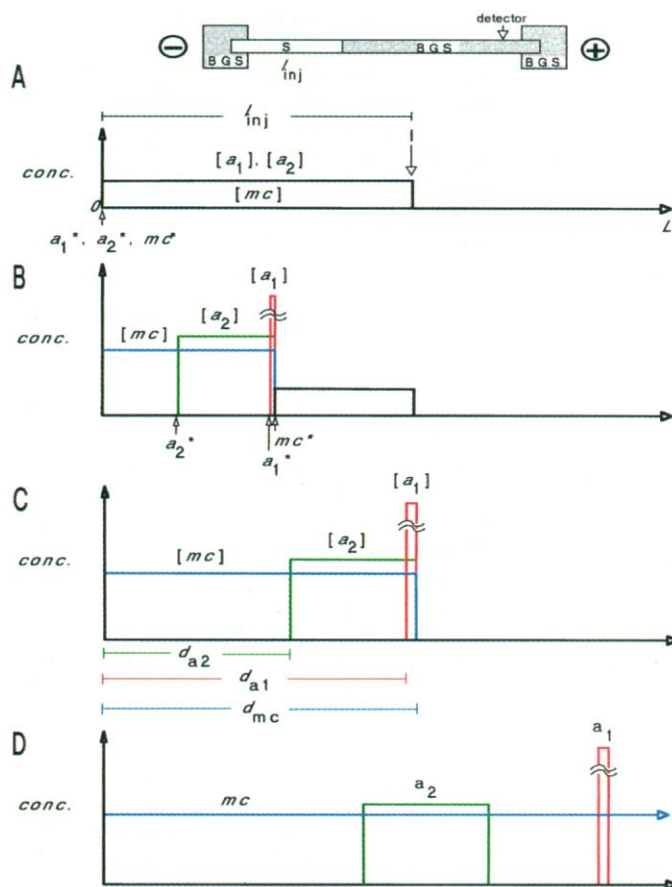


Table 1. Sweeping enhancement factors of several test analytes (11).

Compound	Factor	Compound	Factor
Alkyl phenyl ketones		Heptanophenone	215
Valerophenone	88	Docecanophenone	836
Octanophenone	542		
Naphthalene derivatives and phenanthrene		1-Naphthalene ethanol	113
Naphthalene	92	Phenanthrene	259
1-Nitronaphthalene	168		
Dialkyl phthalates		Diallyl phthalate	337
Diisopropyl phthalate	272	Diisodecyl phthalate	691
Dinonyl phthalate	481		
Steroids		Fluocinolone	1784
Betamethasone	2199	Progesterone	2564
Testosterone	1541		
Some biologically active compounds		Nicardipine	3312
Reserpine	4402	Trimipramine	4727
Quinine	5044		

REPORTS

$$C_{\text{sweep}} = C_{\text{inj}}(1 + k) \quad (3)$$

where C_{inj} is the concentration of the injected zone. In effect, provided $k = 1000$, peak heights obtained from a 64-cm plug of S diluted 1000 times should be equal to that obtained from a 0.64-mm plug (usual injection in EKC) of S. When k is so high, peak heights might be greater in sweeping conditions because the zones are narrowed enormously, but the number of molecule injections is the same. The sample solution in Fig. 3A was diluted 10,000-fold but, injected over a much longer time (about 660) than usual

(Fig. 3B), produced peak heights about one-half that from the usual injection of the original sample solution (Fig. 3A). The k values of these analytes are >1000 using Eq. 3, which is reasonable, because these are very hydrophobic and should have strong affinities toward SDS micelles. In experiments with BGS containing only SDS (no organic modifier), only one peak was observed.

Table 1 lists the sensitivity enhancements gauged as sweeping enhancement factors in terms of peak height obtained with a number of compounds. As predicted by Eq. 3, sensitivity enhancement increases with the increase in k . Deviations can be attributed to the adsorption of the analytes on the capillary walls. Improvements from more than 100 to about 5000-fold were realized for the more hydrophobic solutes. Ghost peaks might appear under sweeping conditions (see Figs. 2 and 3B) and are probably due to isotachophoretic focusing of ions or impurities in the sample solution. Also, there may be changes in the baseline caused by the difference in absorbance levels between S and BGS, which usually appear before the peaks of interest.

Table 2 lists the detection limits, average plate numbers, and reproducibility data for analysis of selected steroids by the sweeping technique. Detection limits are now lower compared with high-performance liquid chromatography. Plate numbers are still impressive and reproducibility and linearity of response are acceptable.

A single and selective clean-up step is recommended to prevent unwanted constituents of the sample matrix to interfere with the analysis. However, for relatively clean liquid samples, the sample conductivity could simply be adjusted to that of the BGS, and the resulting solution could be filtered and directly injected into the capillary (Fig. 4). In theory, one can use much longer capillaries to obtain higher gains in sensitivity. However, this will result in increased analysis time, and commercial instruments are normally capable of delivering voltages up to only 30 kV (10). Applicability of the principle is expected to be usable for larger-scale formats of EKC and not limited to the capillary format.

References and Notes

1. S. Terabe, *Trends Anal. Chem.* **8**, 129 (1989).
2. D. B. Craig, J. C. Y. Wong, N. J. Dovichi, *Anal. Chem.* **68**, 697 (1996).
3. T. J. Thompson, F. Foret, P. Vouros, B. L. Karger, *ibid.* **65**, 900 (1993).
4. R. L. Chien and D. S. Burgi, *ibid.* **64**, 489A (1992).
5. Z. Liu et al., *J. Chromatogr. A* **673**, 125 (1994); K. R. Nielsen and J. P. Foley, *ibid.* **686**, 283 (1994); J. P. Quirino and S. Terabe, *ibid.* **781**, 119 (1997); *ibid.* **791**, 255 (1997); *ibid.* **798**, 251 (1998); *Anal. Chem.* **70**, 149 (1998); *ibid.*, p. 1893; J. P. Quirino, K. Otsuka, S. Terabe, *J. Chromatogr. B* **714**, 29 (1998).
6. S. Terabe, K. Otsuka, K. Ichihara, A. Tsuchiya, T. Ando, *Anal. Chem.* **56**, 111 (1984).
7. All experiments were performed with a Hewlett-

Fig. 2. Effect of retention factor on peak shapes with sweeping. Conditions: BGS, 50 mM SDS in 50 mM phosphoric acid (pH 1.9) containing 20% methanol; S, progesterone (1), testosterone (2), fluocinolone (3), betamethasone (4), hydrocortisone (5), cortisone (6), triamcinolone (7) in phosphoric acid containing 3% methanol, with conductivity similar to BGS; concentration of analytes, about 100 ppb; length of injected S, 16.5 cm; applied voltage, -30 kV.

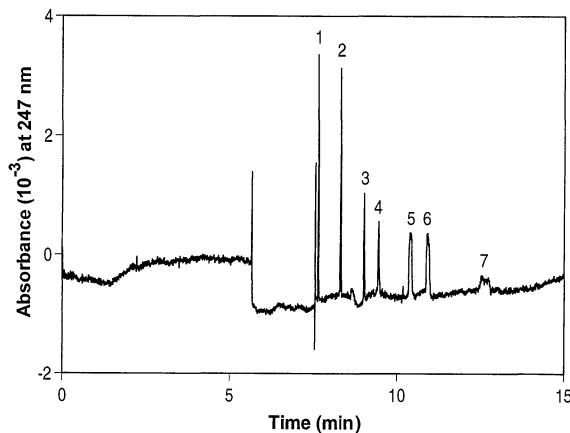


Fig. 3. Optimized electropherogram of selected biologically active compounds with sweeping and comparison with usual injection. Conditions: BGS, 100 mM SDS in 100 mM phosphoric acid (pH 1.9) containing 20% acetonitrile and 2% methanol; S, trimipramine (1), nicardipine (2), noscapine (3), laudanosine (4) in phosphoric acid, with conductivity similar to BGS; concentration of analytes, 190 to 265 ppm (A), 19 to 26.5 ppb (B); length of injected S, 0.064 cm (A), 42 cm (B); applied voltage, -23 kV.

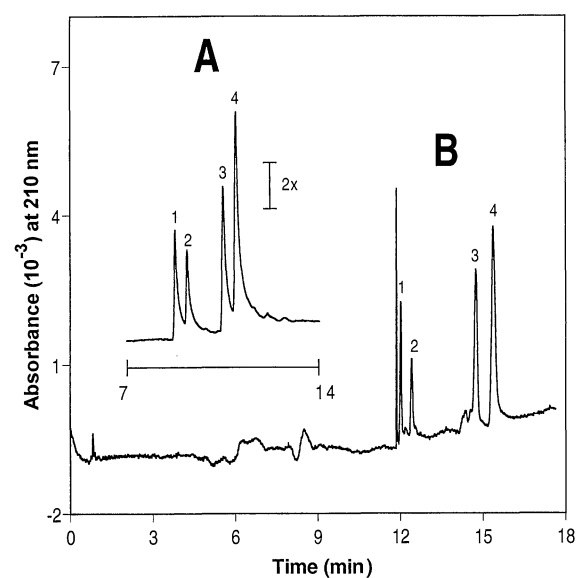


Fig. 4. Low concentration detection and separation of a racemic herbicide spiked in lake water. Conditions: BGS, 50 mM SDS, and 15 mM γ -cyclodextrin (shape selector) in 40 mM phosphoric acid (pH 2); S, fenoprop (f) in lake water adjusted to conductivity of BGS using 500 mM phosphoric acid; final concentration, 9 ppb (first peak under bar), 18 ppb (second peak); injected length, 21 cm; applied voltage, -18 kV.

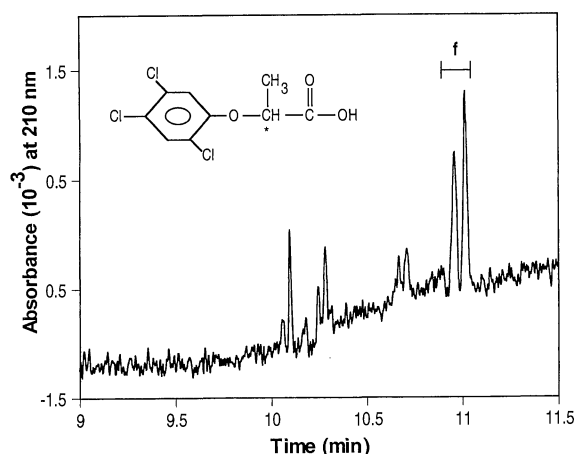


Table 2. Detection limits, RSD(%), and plates of selected steroids with sweeping (12).

Steroids	Progesterone	Testosterone	Fluocinolone	Dexamethasone
Equation of line	$y = 1.27x - 1.58$	$y = 1.18x - 1.34$	$y = 1.00x - 1.32$	$y = 0.89x - 0.98$
Coefficient of variation	$r^2 = 0.9890$	$r^2 = 0.9866$	$r^2 = 0.9859$	$r^2 = 0.9982$
Limit of detection (ppb)	2.6	1.7	1.8	9.6
RSD(%)				
Migration time	0.3	0.3	0.3	0.3
Peak height	13.8	3.9	6.9	8.5
Corrected area	9.4	3.7	4.8	5.3
Plates	1.3×10^6	8.1×10^5	4.9×10^5	9.4×10^4

Packard 3D capillary electrophoresis system equipped with a capillary (50- μ m inside diameter, 56 cm to the detector, and 64.5 cm total length) thermostated at 20°C. Burning off a 3-mm portion of the polyimide capillary coating formed the detection window.

8. The value of *k* was computed for phenanthrene as

marker of the micelle and with the equation $t_{mc}/(t_r - t_{mc})$, where t_{mc} and t_r are the migration times of the marker and analyte, respectively.

9. The trend of Eq. 2 was not verified for the higher *k* values, because accurate determination of *k* when values are very high (>100) is difficult. This is be-

cause elution occurs rapidly (peak compression) and no separation occurs without the addition of aqueous-phase modifiers to the BGs.

10. With 2-m-long capillaries and applied voltage at -30 kV, migration times were more than 1 hour.

11. Sweeping enhancement factor = peak height obtained with sweeping/peak height obtained with usual injection (1 or 2 s at 50 millibars). Supplementary material is available at www.sciencemag.org/feature/data/983374.shl.

12. Conditions: injected length of *S*, 42 cm; other conditions are the same as in Fig. 2; equation of the line, $\log(\text{ppb}) = (\text{slope}) \times \log(\text{mAU}) + y$ intercept; calibration concentration range, 10 to 100 ppb; limit of detection, signal/noise ratio = 3; %RSD (*n* = 7).

13. We thank Drs. K. Otsuka and N. Matsubara for support. J.P.Q. is also grateful to the Ministry of Education, Science, Culture, and Sports, Japan (Monbusho) for a Ph.D. scholarship. Supported in part by grants-in-aid for scientific research (nos. 07554040 and 09304071) from Monbusho.

24 June 1998; accepted 16 September 1998

Increased Vascularization in Mice Overexpressing Angiopoietin-1

Chitra Suri, Joyce McClain, Gavin Thurston, Donald M. McDonald, Hao Zhou, Eben H. Oldmixon, Thomas N. Sato, George D. Yancopoulos*

The angiopoietins and members of the vascular endothelial growth factor (VEGF) family are the only growth factors thought to be largely specific for vascular endothelial cells. Targeted gene inactivation studies in mice have shown that VEGF is necessary for the early stages of vascular development and that angiopoietin-1 is required for the later stages of vascular remodeling. Here it is shown that transgenic overexpression of angiopoietin-1 in the skin of mice produces larger, more numerous, and more highly branched vessels. These results raise the possibility that angiopoietins can be used, alone or in combination with VEGF, to promote therapeutic angiogenesis.

Vascular development can be divided into an early stage (vasculogenesis) and a later stage (angiogenesis) (1). During vasculogenesis, endothelial cells differentiate, proliferate, and coalesce to form a primitive vascular network. Subsequently, this network is transformed into the mature vasculature through angiogenic remodeling processes that involve the sprouting, branching, pruning, and differential growth of vessels, as well as the recruitment of supporting cells.

Two families of growth factors are thought to be largely specific for the vascular endothelium, because expression of their receptors is mainly restricted to endothelial cells (2, 3). These factors include VEGF and its relatives, which are required for vasculogenesis, and the angiopoietins, which appear to be involved in later stages of vessel growth and remodeling. The inactivation of the gene for VEGF or its receptor (VEGFR2) in mice disrupts vascular development at an early stage when endothelial cells begin to differentiate and proliferate (4-6). When angiopoietin-1 (Ang1) or its receptor (Tie2) is inactivated in mice (7-9), the embryos die from the defects in vascular remodeling that occur subsequent to vascular network formation. A factor related to Ang1 (Ang2) apparently acts as a natural antagonist of Tie2 by blocking receptor activation by Ang1 (10). Consistent with this concept, transgenic overexpression of Ang2 results in embryonic lethality due to vascular defects that are similar to those

occurring in the absence of Ang1 or Tie2 (10).

In vitro studies support the notion that Ang1 and VEGF have distinct and complementary roles; Ang1 is not as effective as VEGF in the induction of endothelial cell proliferation or tubule formation in culture, although it can induce sprouting and branch-like phenomena (3, 11). In addition to such remodeling actions, Ang1 may be required for vessel survival or stabilization (9). However, there is no direct evidence that excess Ang1 can promote angiogenesis and vascular remodeling in vivo.

To determine the effects of localized Ang1 overexpression, we generated transgenic mice that overexpressed the protein in their skin. An expression cassette was constructed in which the *Ang1* cDNA was placed under the control of the keratin 14 (K14) gene promoter and enhancer elements (Fig. 1A), which have been previously used to direct gene expression to the skin (12). In transgenic mice that harbor the K14-*Ang1* cassette, skin tissue contained about 12 times the normal amount of Ang1 mRNA (Fig. 1B). In situ hybridization analysis showed that the transgenic transcript was localized to the basal keratinocyte layer of the epidermis as well as to the keratinocytes that line hair follicles (Fig. 1C).

Transgenic mice overexpressing Ang1 appeared generally healthy, as they gained weight and bred normally. However, the skin of these mice appeared strikingly different from that of the control mice. The newborn transgenic mice had many more large blood vessels in their skin (Fig. 2A). The skin of older transgenic mice was markedly redder than normal and became progressively redder from the ages of 2 weeks to 2 months (Fig. 2, B to D), indicating that transgenic Ang1 continued to have effects during postnatal growth.

Distinctive changes in the microvasculature were evident in whole mount preparations of the skin of adult mice, in which vessels were

C. Suri, J. McClain, H. Zhou, G. D. Yancopoulos, Regeneron Pharmaceuticals, 777 Old Saw Mill River Road, Tarrytown, NY 10591, USA. G. Thurston and D. M. McDonald, Department of Anatomy and Cardiovascular Research Institute, University of California, San Francisco, CA 94143, USA. E. H. Oldmixon, Rogers Imaging, Needham, MA 02192, USA. T. N. Sato, University of Texas, Southwestern Medical Center, Dallas, TX 75235, USA.

*To whom correspondence should be addressed. E-mail: gdy@regpha.com